


Dehydrogenation of ethanol over carbon-supported Cu–Co catalysts modified by catalytic chemical vapor deposition

Ekaterina A. Ponomareva^{1,2} · Irina V. Krasnikova³ ·
Ekaterina V. Egorova¹ · Ilya V. Mishakov^{3,4} · Aleksey A. Vedyagin^{3,4} 

Received: 9 June 2017 / Accepted: 11 July 2017 / Published online: 14 July 2017
© Akadémiai Kiadó, Budapest, Hungary 2017

Abstract A bimetallic copper–cobalt catalyst supported on activated carbon fibrous (ACF) material was prepared by the incipient wetness impregnation of the support with an aqueous solution of corresponding nitrates. Reference monometallic Cu/ACF and Co/ACF samples were synthesized analogously. In order to enhance the metal–support interaction and stabilize the dispersion of active components, the Cu–Co/ACF catalyst was subjected to catalytic chemical vapor deposition of ethylene at 600 °C with the formation of carbon nanofibers (CNF). As a result, the catalytic system consisting of Cu–Co particles anchored on carbon–carbon composite was obtained. All samples were characterized by a set of physicochemical methods. The catalytic performance of pristine and CNF-modified samples was studied in the ethanol dehydrogenation reaction. The activity of Cu–Co/CNF/ACF catalyst was shown to be two times higher compared with the unmodified bimetallic sample.

Keywords Ethanol dehydrogenation · Copper–cobalt catalyst · Activated carbon fibers · CCVD · Carbon nanofibers · Carbon–carbon composite

✉ Aleksey A. Vedyagin
vedyagin@catalysis.ru

¹ Institute of Fine Chemical Technologies, Moscow Technological University, Pr. Vernadskogo, 86, Moscow, Russian Federation 119571

² Vernadsky Institute of Geochemistry and Analytical Chemistry RAS, Kosygina str., 19, Moscow, Russian Federation 119991

³ Boreskov Institute of Catalysis SB RAS, pr. Ac. Lavrentieva, 5, Novosibirsk, Russian Federation 630090

⁴ National Research Tomsk Polytechnic University, Lenin Av., 30, Tomsk, Russian Federation 634050

Introduction

Nowadays, the development of industrial processes involving conversion of renewable resources (bio-ethanol, etc.) is of great importance [1]. From this point of view, the catalytic dehydrogenation of ethanol attracts much attention due to formation of acetaldehyde, which is considered as an important intermediate of modern organic chemistry (production of butanol, acetic anhydride, ethyl acetate).

Usually, such metals as platinum, palladium, nickel, cobalt, iron and copper supported on various oxide carriers are used for the catalytic processing of alcohols. Among them, copper-containing catalysts were shown to be most selective towards target product [2]. On the other hand, bimetallic catalysts having unique structural, electronic and chemical properties demonstrate superior catalytic performance [3]. Thus, copper–cobalt catalysts for Fischer–Tropsch synthesis are known to perform much higher activity comparing with cobalt-only ones [4, 5].

Besides the effect of the active component, the catalytic properties might be significantly influenced by the nature of the support and its surface properties. All this determines the strength of metal–support interaction, which, in turn, affects the thermal stability of the system including the chemical state of the active component and the possibility of agglomeration processes. Compared with oxide supports, carbon materials provide high thermal conductivity, mechanical strength, developed porous structure, and appropriate chemical resistance [6]. The interaction of the supported metals with carbon support is rather weak. Thus, no surface intermediates complicating the reduction of metals and worsening the catalytic activity and selectivity of the dehydrogenation process are being formed [5, 7, 8].

It should be mentioned that the shape of the catalyst also plays an important role on its catalytic performance. Thus, the application of powders and small granules is limited due to their possible removal from the reactor by reaction flow. Another known drawback is a pressure drop of fixed-bed catalyst. The use of cloth-shaped catalysts can alternatively solve the problems pointed above. An appropriate geometrical structure and flexibility of cloth materials open new possibilities to be applied in reactors of any design including scaled-up and industrial ones [9, 10].

Taking all said into account, in present work, we have used cloth-shaped activated carbon fibers (ACF) as a support for bimetallic copper–cobalt catalyst of ethanol dehydrogenation. The developed surface area of such carbon fibers (up to $1000 \text{ m}^2 \text{ g}^{-1}$) allows one to prepare finely dispersed particles of active component. At the same time, it was reported earlier that carbon-supported copper particles undergo noticeable agglomeration under dehydrogenation conditions in a temperature range of 200–400 °C [8, 11]. The presence of water vapor in a reaction mixture may also influence the chemical state of active component [12]. In order to avoid these undesired effects, carbon–carbon composite materials of hierarchical structure can be applied as a support [13, 14]. Most commonly, such composite materials are derived via the catalytic chemical vapor deposition (CCVD) of different hydrocarbons [15, 16]. This approach includes the deposition of corresponding active components on the surface of macrostructured carbon followed by the decomposition of hydrocarbon with the formation of carbon

nanofibers (CNF). Thereby, in the present work, we have compared the physico-chemical and catalytic properties of Cu–Co/ACF catalyst with Cu–Co/CNF/ACF, which was obtained by the CCVD of ethylene over Cu–Co/ACF.

Experimental

Synthesis of the samples

Cloth-shaped activated carbon fibers (AW1101, Taiwan Carbon Technology Co.) characterized by high specific surface area ($SSA = 1055 \text{ m}^2 \text{ g}^{-1}$) and microporous structure ($V_{\text{micro}} = 0.31 \text{ cm}^3 \text{ g}^{-1}$) were used as a support. The samples were prepared by the incipient wetness impregnation of ACF with an aqueous solution of corresponding nitrates ($\text{Cu}(\text{NO}_3)_2 \cdot 3\text{H}_2\text{O}$ and $\text{Co}(\text{NO}_3)_2 \cdot 6\text{H}_2\text{O}$) followed by drying at $110 \text{ }^\circ\text{C}$ for 1 h. Then, the samples were calcined at $350 \text{ }^\circ\text{C}$ for 30 min in an argon flow and reduced in hydrogen at $600 \text{ }^\circ\text{C}$ for 15 min. The total metal loading was 5 wt%. In the case of bimetallic catalyst, the metal ratio was 1:1. The samples were labeled as Cu–Co/ACF, Cu/ACF and Co/ACF.

The catalytic chemical vapor deposition of ethylene was performed over Cu–Co/ACF sample at $600 \text{ }^\circ\text{C}$ in a flow-through quartz reactor equipped with McBain balances. The duration of the CCVD process was 2 min, which corresponds to about 6 wt% yield of carbon nanofibers. The sample was labeled as Cu–Co/CNF/ACF.

Characterization of the samples

Monometallic Cu/ACF and Co/ACF, and bimetallic Cu–Co/ACF samples after calcination were studied by temperature-programmed reduction in hydrogen (TPR- H_2). A thermal conductivity detector was used to measure the hydrogen concentration. In each experiment, the sample (100 mg) was placed into the reactor, preheated at $300 \text{ }^\circ\text{C}$ for 1 h in argon, and then cooled down to room temperature. Then, the sample was heated up to $850 \text{ }^\circ\text{C}$ with ramping rate of $10 \text{ }^\circ\text{C min}^{-1}$ in a flow (30 ml min^{-1}) containing 5 vol% of hydrogen in argon.

The samples were characterized by X-ray diffraction analysis (XRD) on a DRON-3 diffractometer using Cu K_α radiation ($\lambda = 0.154 \text{ nm}$) at an operating voltage of 40 kV. The XRD patterns were recorded in a range of 30° – 60° . Phase analysis was performed in accordance with PCPDFWIN v2.02 database. The value of coherent-scattering region (CSR) was determined using the Scherrer equation.

Transmission electron microscopy (TEM) study was carried out on a JEM 1400 (Jeol, Japan) microscope at an accelerating voltage of 80 kV. An especially designed technique of sample pretreatment and holding was used to visualize the nano/microfibers interface [16].

Testing the catalytic activity in ethanol dehydrogenation

The catalytic activity of the prepared samples was studied in the ethanol dehydrogenation reaction. The experiments were carried out in a fixed-bed quartz

reactor (10 mm i.d.) at atmospheric pressure within the temperature range of 200–400 °C. The reaction mixture (93 wt% of ethanol in water) was fed into the reactor with preloaded sample (0.47 ml) at a gas hourly space velocity (GHSV) of 32 h⁻¹. The composition of a reaction mixture was analyzed by means of gas chromatography (GC) equipped with Porapak-Q column.

Results and discussion

Since the oxidation state of active metals affects both the realization of the CCVD process and the catalytic behavior in ethanol dehydrogenation, the Cu–Co/ACF, Cu/ACF and Co/ACF samples after the calcination procedure were studied by means of temperature-programmed reduction. The resulting profiles are shown in Fig. 1. The reduction behavior of the samples is known to be related to the size of copper and/or cobalt species, and the strength of metal-support interaction [17, 18]. Thus, in the case of the Cu/ACF sample, the reduction of copper occurs in two steps within the temperature range of 150–350 °C. The first intensive hydrogen consumption at 200–220 °C can be assigned to the reduction of finely dispersed or surface copper species, while the peak at 300 °C corresponds to the reduction of bulk copper oxide [19]. TPR-H₂ profile for Co/ACF sample is much broader, and lies in the temperature range of 160–640 °C. According to the literature, oxidized cobalt also undergoes stepwise reduction with regard to the following scheme: Co₃O₄ → CoO → Co [20, 21]. In the case of carbon-supported catalysts, the situation might be more complicated. Such processes as hydrogen interaction with the surface oxygen-containing groups of the support and even its partial gasification can take place in a temperature interval of 400–600 °C [22–24]. At the same time, pure activated carbon fibers (with no metal supported) examined under the same TPR conditions show no noticeable hydrogen consumption up to 800 °C.

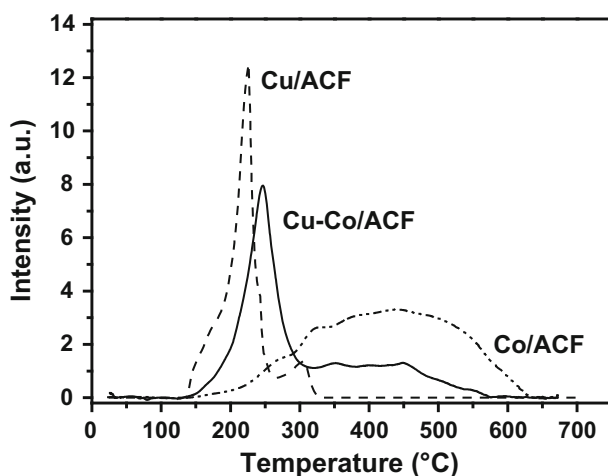


Fig. 1 TPR-H₂ profiles for Cu–Co/ACF, Cu/ACF and Co/ACF samples

The pattern for the Cu–Co/ACF sample represents a number of overlapped peaks, which correspond to the reduction of different metals in a wide temperature range (150–570 °C). An intensive peak at 250 °C is attributed to the reduction of dispersed copper species. At the same time, the broadening of the peaks within range of 200–400 °C indicates the presence of mixed Cu–Co oxides [25]. As can be seen from the comparison of TPR-H₂ profiles for monometallic and bimetallic catalysts, the reduction of oxidized copper in the Cu–Co/ACF sample occurs at a higher temperature (250 instead of 220 °C for Cu/ACF), whereas the reduction of cobalt is completed at temperature 50 °C lower than that for pure Co/ACF. This synergetic effect taking place during the hydrogen treatment of bimetallic catalysts is well known in the literature [5, 24, 26].

The samples before and after the reaction of ethanol dehydrogenation were characterized by means of XRD analysis. Fig. 2 demonstrates the corresponding patterns. Table 1 summarizes the calculated values of coherent-scattering regions for the studied samples. The Cu–Co/CNF/ACF sample was used as-prepared, while all other ACF-based samples were examined after preliminary reduction. As follows from Fig. 2, copper in the monometallic Cu/ACF sample is represented by the oxide phase only, which is connected with weak metal-support interaction and facilitated the oxidation of dispersed copper particles in air. On the other hand, the sample after the reaction also contains metallic copper, thus indicating the agglomeration of the active particles under the reaction conditions. In the case of the Co/ACF catalyst, cobalt was found to be in roentgen-amorphous state. No phases were detected, nor before, nor after the reaction.

Fig. 2 XRD patterns for the samples: 1 Cu–Co/ACF (reduced); 2 Cu–Co/ACF (after reaction); 3 Cu–Co/CNF/ACF (initial); 4 Cu/ACF (reduced); 5 Cu/ACF (after reaction); 6 Co/ACF (reduced)

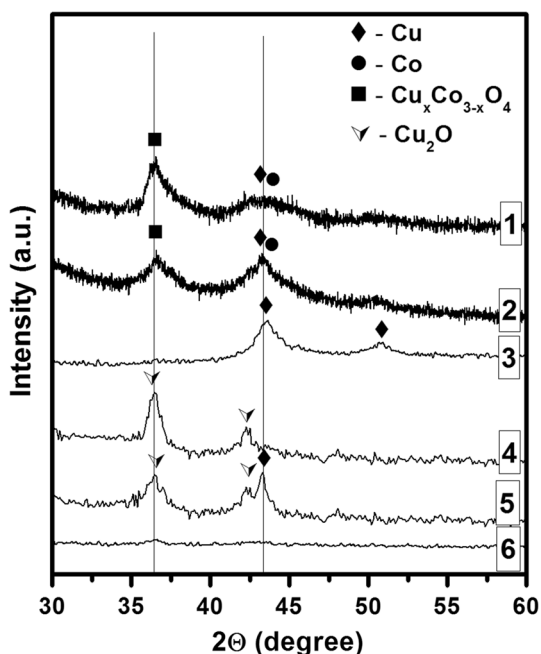


Table 1 Coherent-scattering regions (CSR) calculated in accordance with XRD data

#	Sample	Comments	Phase	CSR (nm)
1	Cu–Co/ACF	After reduction	Cu–Co alloy	7
2	Cu–Co/ACF	After reaction	Cu–Co alloy Cu _x Co _{3–x} O ₄ mixed oxide	14 11
3	Cu–Co/CNF/ACF	Initial	Cu–Co alloy	21
4	Cu–Co/CNF/ ACF	After reaction	Cu–Co alloy	21
5	Cu/ACF	After reduction	CuO	23
6	Cu/ACF	After reaction	Cu CuO	29 18

For the bimetallic Cu–Co/ACF sample, both metal and oxide phases were registered. The appearance of reflections assigned to the Cu_xCo_{3–x}O₄ mixed oxide phase is in good agreement with TPR-H₂ data as well as with the literature [4]. The intensity and width of reflections at 43.3° and 51.3° (corresponding to metallic copper) are different for the samples before and after the reaction, which is also connected with the agglomeration of metal particles occurred during the reaction. As shown in Table 1, the CSR value for this sample after the reaction is increased twofold.

Surprisingly, it was found that the XRD patterns for the CCVD-modified sample before and after the reaction are totally identical. In the case of the Cu–Co/CNF/ACF sample, the active component is represented by bimetallic alloyed particles. The formation of an alloy has shifted the position of the reflection at 43.60° (characteristic for pure copper) to 43.30° (attributed to the corresponding alloy) [27, 28]. Thereby, strong metal-support interaction taking place in the Cu–Co/CNF/ACF sample was found to stabilize the dispersity and the chemical state of active bimetallic particles.

The Cu–Co/CNF/ACF sample was additionally studied by transmission electron microscopy. Fig. 3 presents a general view of CCVD-modified activated carbon fiber and carbon nanofibers grown as a result of CCVD of ethylene over Cu–Co metal particles. The bimodal particle size distribution of active component was observed by TEM (Fig. 3c). The amount of large particles (about 100 nm) does not exceed 23%, while the most part of particles are characterized with much smaller size (near 10 nm). Most probably, the bimodality of particle size is caused by agglomeration/disintegration processes taking place during the preliminary reduction of the Cu–Co/ACF sample and at the beginning of CCVD procedure. It should be also emphasized that the particles of the active component are strongly anchored to the surface of microfibers (ACF), thus providing their stabilized dispersion. The short times of the CCVD process result in a small yield of CNF (6 wt%), which makes the Cu–Co alloyed particles accessible for the reactants in the ethanol dehydrogenation process.

Bimetallic and monometallic reference samples were tested in ethanol dehydrogenation reaction. The catalytic activity was calculated as an amount of converted ethanol in relation to the metal loading during 1 h. The obtained temperature

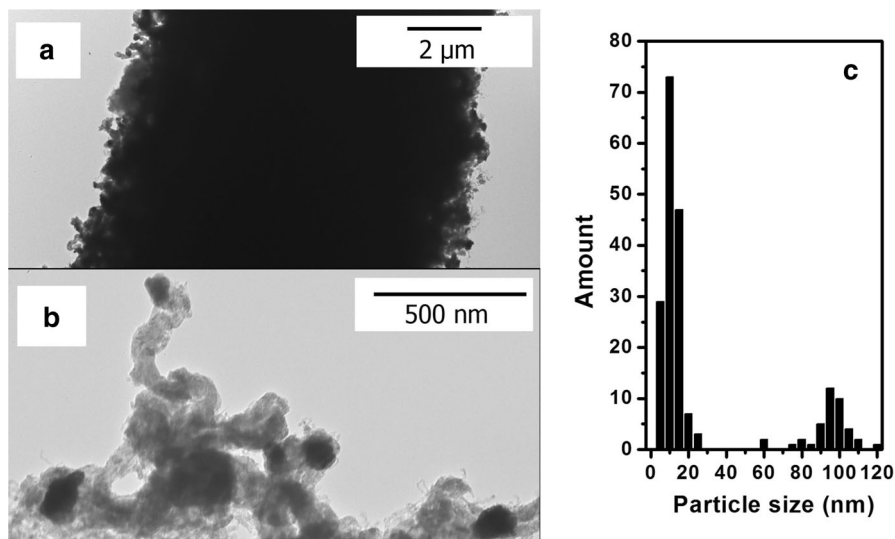


Fig. 3 TEM data for Cu–Co/CNF/ACF sample: **a** general view of CCVD-modified ACF; **b** carbon nanofibers with metal particles; **c** particle size distribution

dependences of the catalytic activity and acetaldehyde yield are shown in Figs. 4, 5 and 6. As seen from Fig. 4, the dependences of the catalytic activity for bimetallic samples are quite complicated. The curves can be symbolically divided into three zones: I and III—ascending dependence, temperature ranges of 200–300 and 355–400 °C, correspondingly; II—descending dependence, temperature range of 300–355 °C. It was suggested that such unusual shape of curves is connected with the different temperature intervals of activity for copper and cobalt. Fig. 5 shows the analogous dependencies for monometallic Cu/ACF and Co/ACF

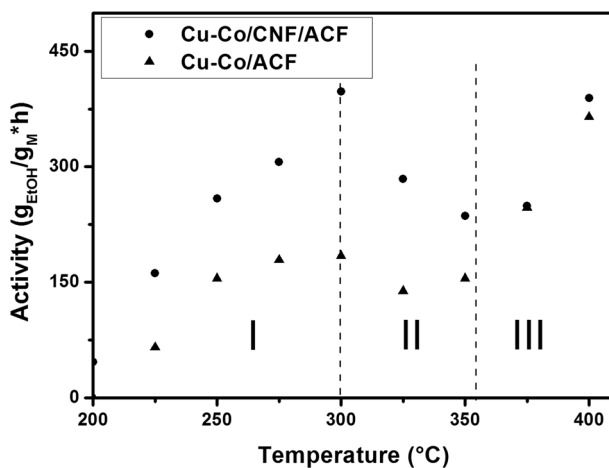


Fig. 4 Temperature dependences of catalytic activity for Cu–Co/ACF and Cu–Co/CNF/ACF samples

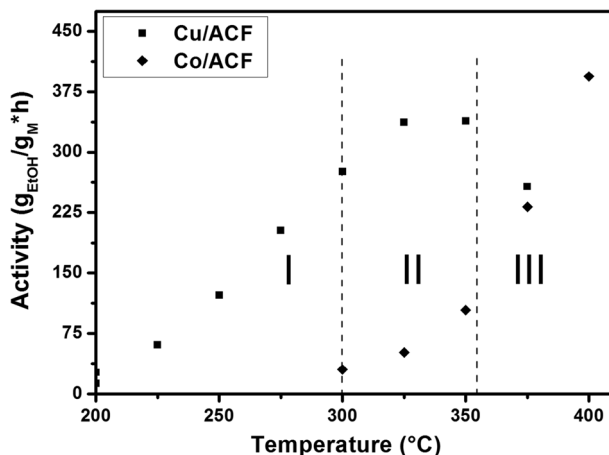


Fig. 5 Temperature dependences of catalytic activity for Cu/ACF and Co/ACF samples

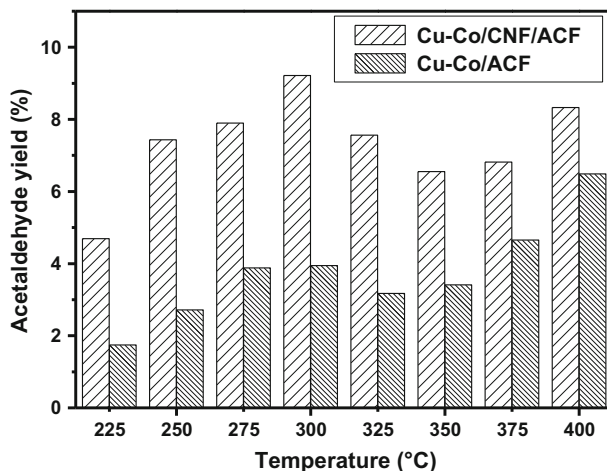
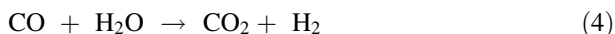
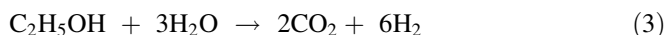


Fig. 6 Acetaldehyde yield versus temperature for Cu–Co/ACF and Cu–Co/CNF/ACF samples

catalysts. As seen, copper is active starting from 200 °C, and activity grows until 350 °C. Cobalt starts to be active at temperatures above 300 °C. Thereby, the shape of temperature dependence curves for bimetallic samples can be assigned to the superposition of copper and cobalt activity. It should be mentioned that activity of the CCVD-modified Cu–Co/CNF/ACF catalyst is two times higher within zone I if compared with the unmodified Cu–Co/ACF sample, and about 1.5 times higher if compared with the monometallic Cu/ACF reference sample.

The selectivity of the ethanol dehydrogenation process was calculated on the basis of GC data. It lies in a range of 90–100 and 80–100% for the Cu–Co/CNF/ACF and Cu–Co/ACF catalysts, accordingly. Among the products, acetaldehyde

and hydrogen prevailed (reaction 1). Nevertheless, side processes also take place (reactions 2–4).



Temperature dependencies of the acetaldehyde yield for the Cu–Co/CNF/ACF and Cu–Co/ACF samples are demonstrated in Fig. 6. The acetaldehyde yield obtained over Cu–Co/CNF/ACF is more than two times higher comparing with Cu–Co/ACF sample. The difference in yield reaches its maximum in the range of 275–325 °C, where the catalytic activity of the system is determined by copper. Copper is known to enrich the surface of bimetallic Cu–Co particle due to its lower surface energy ($\gamma_{\text{Cu}} = 1.85 \text{ J m}^{-2}$; $\gamma_{\text{Co}} = 2.59 \text{ J m}^{-2}$) [29, 30]. During the CCVD process and growth of carbon nanofibers, the faces of active component particles are differentiated with respect to their functions and affinity to carbon. Consequently, cobalt, which has higher affinity to carbon, is represented on the ‘carbon deposition’ face (111), while copper is situated on the exposed sides. Thus, cobalt in the Cu–Co/CNF/ACF system may be partially covered with carbon, while the copper is located on ‘carbon-free’ edges. Such redistribution of active components, as it was demonstrated, affects both the catalytic activity in ethanol dehydrogenation and the yield of acetaldehyde. It can be concluded here that a strong metal-support interaction occurred due to formation of carbon nanofibers stabilizes both the dispersity and chemical state of Cu–Co particles, thus allowing the Cu–Co/CNF/ACF system to perform the superior catalytic activity.

Conclusions

The catalytic activity of bimetallic Cu–Co/ACF and Cu–Co/CNF/ACF samples was studied in the ethanol dehydrogenation reaction. Monometallic Cu/ACF and Co/ACF catalysts were used as a reference. The CCVD-modified Cu–Co/CNF/ACF sample was shown to perform superior catalytic activity. According to TEM data, this sample is characterized with bimodal particle size distribution (10 and 100 nm). Both the dispersity of the particles and their chemical state were found to be stabilized due to the strong metal-support interaction of Cu–Co particles with carbon nanofibers. Thereby, the bimetallic copper–cobalt system supported on carbon–carbon composite is considered as a promising catalyst for the ethanol dehydrogenation process.

Acknowledgements This work was supported by Russian Academy of Sciences and Federal Agency of Scientific Organizations (state-guaranteed order for BIC, Project No. 0303-2016-0014).

References

1. Gallo JMR, Bueno J, Schuchardt U (2014) *J Braz Chem Soc* 25:2229–2243
2. Chladek P, Croiset E, Epling W, Hudgins RR (2007) *Can J Chem Eng* 85:917–924
3. Konsolakis M, Ioakeimidis Z (2014) *Appl Surf Sci* 320:244–255
4. Wang L, Cao A, Lui G, Zhang L, Liu Y (2016) *Appl Surf Sci* 360:77–85
5. Ma WP, Ding YJ, Lin LW (2004) *Ind Eng Chem Res* 43:2391–2398
6. Li J, Tang X, Yi H, Yu Q, Gao F, Zhang R, Li C, Chu C (2017) *Appl Surf Sci* 412:37–44
7. Ampelli C, Perathoner S, Centi G (2014) *Chin J Catal* 35:783–791
8. Morales MV, Asedegbega-Nieto E, Bachiller-Baeza B, Guerrero-Ruiz A (2016) *Carbon* 102:426–436
9. Zazhigalov S, Elyshev A, Lopatin S, Larina T, Cherepanova S, Mikenin P, Zagoruiko A (2017) *React Kinet Mech Cat* 120:247–260
10. Vedyagin AA, Mishakov IV, Tsyrlunikov PG (2016) *React Kinet Mech Cat* 117:35–46
11. Shelepova EV, Vedyagin AA, Ilina LY, Nizovskii AI, Tsyrlunikov PG (2017) *Appl Surf Sci* 409:291–295
12. Fan YJ, Wu SF (2016) *J CO2 Util* 16:150–156
13. Kong Y, Qiu T, Qiu J (2013) *Appl Surf Sci* 265:352–357
14. Ledoux MJ, Pham-Huu C (2005) *Catal Today* 102–103:2–14
15. Sun J, Li H, Feng L, Jia Y, Song Q, Li K (2017) *Appl Surf Sci* 403:95–102
16. Krasnikova IV, Mishakov IV, Vedyagin AA, Bauman YI, Korneev DV (2017) *Mater Chem Phys* 186:220–227
17. Potoczna-Petru D, Kepinski L (2001) *Catal Lett* 73:41–46
18. Sales EA, de Souza TRO, Santos RC, Carvalho Andrade HM (2005) *Catal Today* 107–108:114–119
19. Jeon GS, Chung JS (1994) *Appl Catal A* 115:29–44
20. Zaman M, Khodadi A, Mortazavi Y (2009) *Fuel Process Tech* 90:1214–1219
21. Yang Y, Jia L, Meng Y, Hou B, Li D, Sun Y (2012) *Catal Lett* 142:195–204
22. Pei Y, Ding Y, Zhu H, Du H (2015) *Chin J Catal* 36:355–361
23. Fu T, Huang Ch, Lu J, Li Z (2014) *Fuel* 121:225–231
24. Bai S, Huang C, Lv J, Li Z (2012) *Catal Commun* 22:24–27
25. Baker JE, Burch R, Hibble SJ, Loader PK (1990) *Appl Catal* 65:281–292
26. Chuang KH, Lu CY, Wey MY, Huang YN (2011) *Appl Catal A* 397:234–240
27. Cesar DV, Pérez CA, Salim VMM, Schmal M (1999) *Appl Catal A* 176:205–212
28. Nishizawa T, Ishida K (1984) *J Phase Equilib* 5:161–165
29. Van Stiphout PCM, Stobbe DE, Scheur FTV, Geus JW (1988) *Appl Catal* 40:219–246
30. Roth TA (1975) *Mater Sci Eng* 18:183–192